Equine Veterinary Education

EQUINE VETERINARY EDUCATION
Equine vet. Educ. (2018) •• (••) ••-••
doi: 10.1111/eve.12952

Case Report

Advanced imaging of an incomplete fracture and exostosis of the third metacarpal bone in a young Warmblood horse

***C. M. Isgren*[†‡*], *T. W. Maddox*[§], *R. Blundell*[¶], *M. Sinovich*[†] *and L. M. Rubio-Martinez*[†]**

[†]*Department of Equine Clinical Science, Institute of Veterinary Science, University of Liverpool;* [‡]*Department of Epidemiology and Population Health, Institute of Infection and Global Health, University of Liverpool;* [§]*Department of Musculoskeletal Biology, Institute of Ageing and Chronic Disease, University of Liverpool; and* [¶]*Department of Veterinary Pathology, Infection and Public Health, Institute of Veterinary Science, University of Liverpool, Leahurst, Wirral, UK*

**Corresponding author email: cisgren@liverpool.ac.uk*

Keywords: horse; bone pathology; sclerosis; magnetic resonance imaging; computed tomography; histopathology

Summary

A 5-year-old Hanoverian gelding with acute moderate right forelimb lameness underwent nuclear scintigraphy, which identified marked increase in radiopharmaceutical uptake of the proximomedial aspect of the right metacarpus. Ultrasonography and radiography identified sclerosis and exostosis of the proximomedial aspect of the metacarpal bone III in-between the suspensory ligament and the second metacarpal bone, and presence of a suspected fracture. The owner requested euthanasia of the gelding, and post-mortem computed tomography and magnetic resonance imaging identified marked bone sclerosis and thickening of the palmar cortex of the metacarpal III (McIII), presence of an incomplete fracture in the palmar cortex of McIII and expansive exostosis from McIII extending in a palmar direction between the suspensory ligament and the second metacarpal bone. Histopathological examination confirmed the imaging findings of sclerosis and led to final diagnosis of a fracture of the palmar cortex of the McIII associated with an exostosis encroaching the medial aspect of the suspensory ligament. No abnormalities were present in the suspensory ligament or metacarpal bone II (McII).

Introduction

Incomplete palmar cortical fatigue fractures of proximal metacarpal III (McIII) have been reported in isolation (Dyson 1991; Riggs 1994; Pinchbeck and Kriz 2001; Morgan and Dyson 2012; Beccati *et al.* 2017) as well as concurrently with desmitis of the proximal suspensory ligament (PSL) (Ross *et al.* 1988; Beccati *et al.* 2017). Exostosis of the palmar aspect of the proximal McIII has previously been described without the presence of an incomplete palmar cortical fracture but with concurrent desmitis of the PSL (Launois *et al.* 2009). Injuries in the proximal McIII region can involve the bone and/or suspensory ligament and advanced imaging is pertinent for accurate diagnosis (Beccati *et al.* 2017). The current case report describes an incomplete fracture and exostosis of the proximal palmar McIII without associated SL involvement and, to the authors' knowledge, this is the first description of such a lesion using nuclear scintigraphy, radiography, ultrasonography, CT and MRI.

Case history

A 5-year-old 476 kg Hanoverian gelding, used for showing, was presented for investigation of a moderate right forelimb (RF) lameness of 2-week duration. The referring veterinarian had attempted diagnostic analgesia unsuccessfully due to the horse's temperament.

Clinical findings

Clinical examination was unremarkable, with no pain evident on palpation including the proximal suspensory ligament (PSL). The gelding was sound at walk and a 5/10th RF lameness (Arkell *et al.* 2006) was evident at the trot on a hard surface in a straight line. On the left circle, a 5/10th RF lameness was present and on a right circle a 2/10th RF lameness was evident on both the soft and firm surfaces. An abaxial sesamoid nerve block was attempted but despite sedation this was again unsuccessful due to the gelding's temperament.

Gamma scintigraphic imaging of the both forelimbs, thoracic spine and neck was performed with a gamma camera (Bartec- N-XRD Nucline X-Ring/R Gamma Camera Detector[1]) with bone-phase images obtained 3 h after injection of technetium-99-DP (10 MBq/kg [4.5 MBq/lb], i.v.). This identified markedly increased focal radiopharmaceutical uptake (IRU) of the proximomedial aspect of the right metacarpus with approximately four times the activity of the equivalent region of the contralateral limb (**Fig 1**). Following isolation, lateromedial, dorsopalmar, dorsomedial palmarolateral and dorsolateral palmarolateral oblique radiographic projections of the proximal metacarpus were obtained (Magnum C-DMS[2]: settings 80 kV and 5 mAs). An approximately 3 cm radiolucent line was identified at the proximomedial aspect of McIII extending from 4 mm distal to the carpometacarpal joint in the palmar cortex in a proximolateral to distomedial direction (**Fig 2**). Increased radiopacity consistent with sclerosis was present abaxial to the radiolucent line and axial to metacarpal II (McII) and this area contained poorly defined horizontal radiolucent lines. The axial margin of McII had an irregular and poorly defined outline and appeared continuous with the area of increased radiopacity. Weightbearing and nonweightbearing ultrasonographic examination (linear probe, 10 MHz, Logic E[3]) identified a well-defined protruding structure with a

hyperechogenic irregular outline in between the medial border of the PSL and continuous with McII, which obscured the normal contour of the axial margin of McII (**Fig 2**). This area was consistent with mineralised tissue and appeared continuous with the axial aspect of McII. The PSL was deviated laterally as a consequence of this space-occupying mineralised area and had a normal heterogeneous echogenicity throughout, with well-defined margins.

Diagnosis

Based on radiographic and ultrasonographic findings, differential diagnosis included an incomplete fracture of the palmar aspect of proximomedial McIII with irregular new periosteal bone formation, or fracture of the axial aspect of the McII with callus formation.

Post-mortem imaging and histopathology

The owner declined further diagnostics or treatment despite being given a favourable prognosis with conservative management. The owner requested for the gelding to be subjected to euthanasia due to personal circumstances and the difficult temperament of the horse. Following euthanasia, the limb was transected proximal to the carpus and computed tomography (CT) of the distal limb was performed (Lightspeed VCT 4 Slice[3]) with the following technical parameters: 120 kV [peak], 155 mAs, 1.25 mm contiguous slices. Bone and soft tissue algorithms were used with an image field of view (FOV) of 110 mm diameter and matrix dimensions of 512 × 512. CT revealed poorly marginated sclerosis of the palmaromedial aspect of proximal McIII in the region of and adjacent to the origin of suspensory ligament, with a small, sharply defined exostosis (moderately hypoattenuating compared to cortical bone) extending from the palmaromedial cortex of McIII in a palmar direction and partially encroaching the medial margin of the suspensory ligament (**Fig 3**). Associated with this was a fine, linear and well-defined hypoattenuating region (approximately 30 mm) consistent with a fracture orientated proximodistally through the palmar cortex of McIII. It was located 4 mm distal to the carpometacarpal joint and did not enter the articular surface. There was a

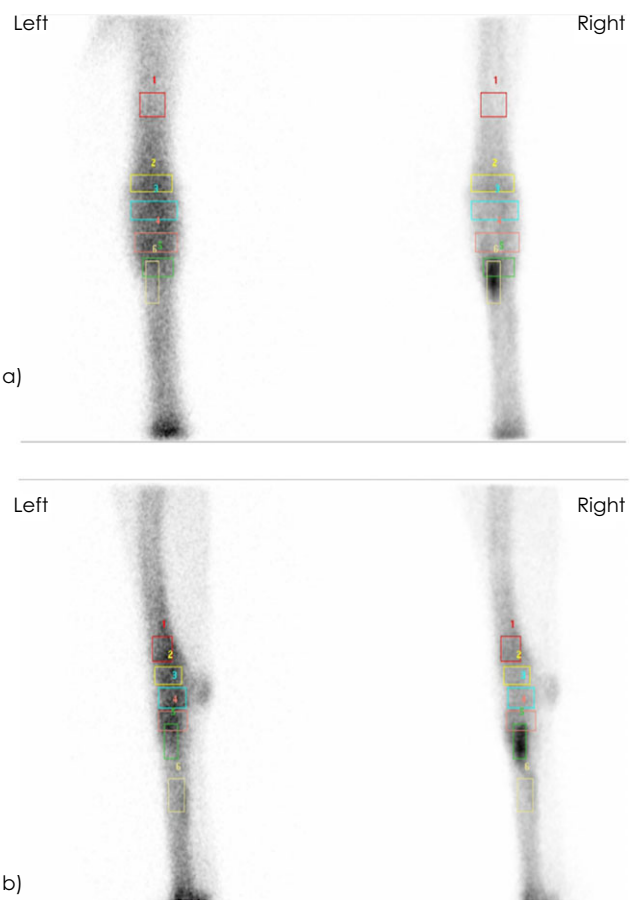

Fig 1: Gamma scintigraphy corrected multimodality images. a) Dorsal to palmar projection of both carpi showing a four-fold increase in focal radiopharmaceutical uptake of the proximomedial aspect of the right metacarpus compared to the left. b) Lateral to medial projection.

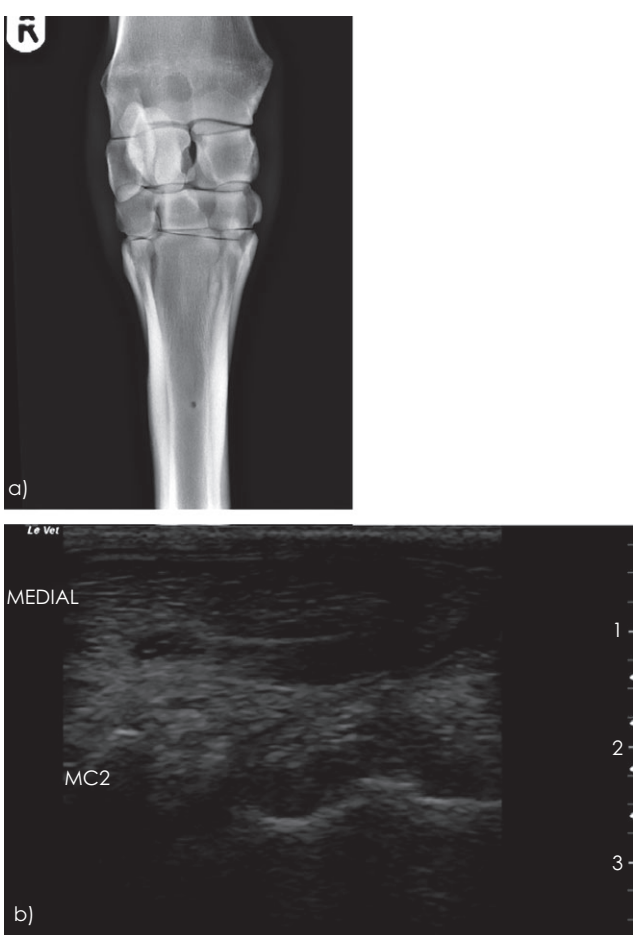

Fig 2: a) Dorsal to palmar radiographic projection. This view shows the radiolucent line extending from distal to the carpometacarpal joint, in the palmar cortex in a proximolateral to distomedial direction. b) Longitudinal ultrasonographic view of a well-defined, prominent, hyperechogenic structure with an irregular outline, between the medial border of the proximal suspensory ligament and continuous with McIII.

smooth periosteal reaction of the dorsomedial cortex of proximal McIII at same level. Magnetic resonance imaging (MRI) was performed using a 1T scanner (Siemens Magnetom[4]), with images obtained in two planes (dorsal and transverse) and included T2* gradient echo (TR/TE 1270/26 ms, NEX 3), short tau inversion recovery (STIR) (TR/TE 5000/110 ms, inversion time 150 ms, NEX 1), T1- (TR/TE 652/14 ms, NEX 4) and T2-weighted (TR/TE 3000/100 ms, NEX 5) fast spin echo sequences with a FOV of 140 × 140 mm, acquisition matrix of 256 × 256, 4 mm slice thickness and 4 mm slice gap. The well-defined palmar cortical defect was represented by a linear hyperintensity on T2* gradient echo, STIR, T1- and T2-weighted sequences, with surrounding hypointensity on all sequences within the palmaroproximal aspect McIII (consistent with bone sclerosis) (**Fig 3**). STIR images showed a small area of high signal adjacent to the sclerotic region within proximal McIII. The PSL had a regular appearance apart from a slight lateral deviation due to presence of the low signal intensity exostosis medially, whilst McII was unaffected. Advanced imaging provided information about the extent of the fracture and size and shape of the exostosis. The advanced imaging diagnosis was incomplete fracture associated with sclerosis of the palmar aspect of proximomedial McIII and irregular exostosis.

Gross post-mortem examination revealed that the compact cortical bone of the palmar medial aspect of McIII was thickened and encroached into the central trabecular bone. There was a bony exostosis (~10 × 5 mm) immediately abaxial to the suspensory ligament and axial to the McII protruding from the palmar surface of McIII. Histopathological examination of the proximal McII, McIII and the PSL revealed an expanded area of focally extensive osteonal bone of the palmar cortex invading the trabecular bone dorsally (**Fig 4**). The bone exhibited a moderately irregular pattern of osteon formation, which was variably sized and irregularly shaped. The osteonal bone within the lesion was very dense, with wide bands of bony extracellular matrix and irregular osteonal architecture of variably sized haversian canals. There were often multiple haversian canals per osteon. This area was continuous with the more regular osteonal bone, which represented less affected bone further dorsally. The bone also extended into an exophytic bony projection in a palmar direction, consistent with an exostosis, which was composed of well-differentiated woven bone. The suspensory ligament and McII were unremarkable on all examined sections. The histological findings represent an area of osteosclerosis of McIII and a small exostosis likely related to the same lesion. The fracture was not evident on histopathology due to

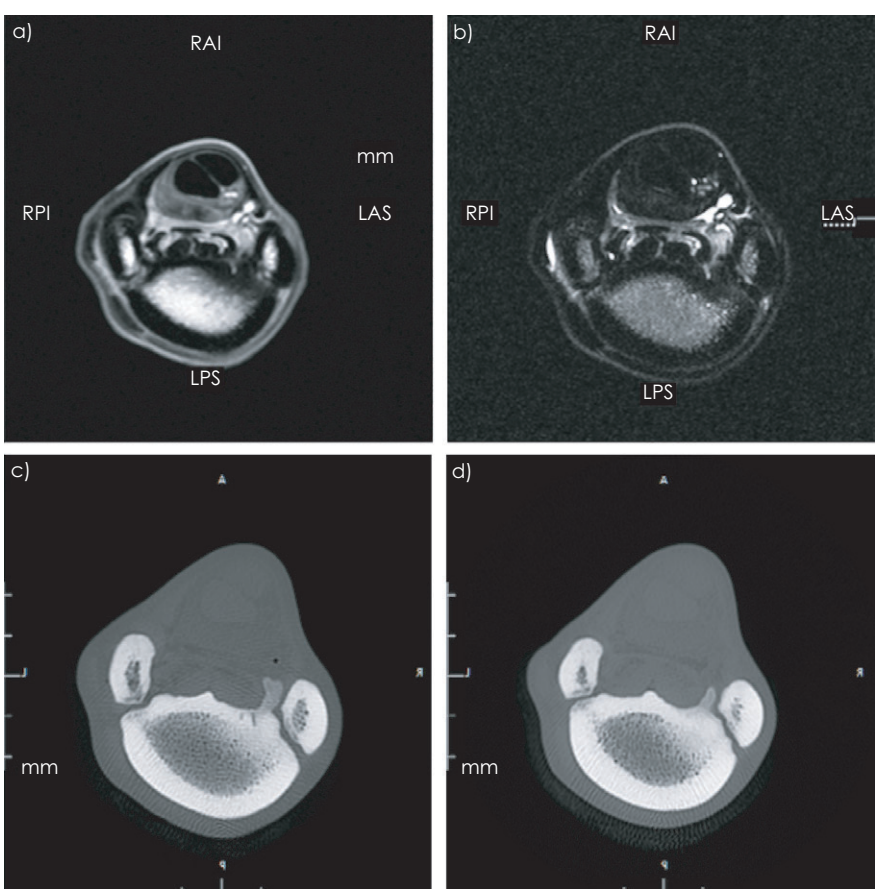

Fig 3: T1W transverse MRI image (a) and T2W (b) transverse MRI image showing the cortical defect as a well linear hyperintensity. c) Transverse CT image. A linear, hypoattenuating region, consistent with a fracture was present, which orientated proximodistally through the palmar cortex of McIII. d) Transverse CT image. A focal area of poorly marginated sclerosis was present on the palmaromedial aspect of proximal McIII showing a sharply defined exostosis extending from the palmaromedial cortex of McIII in a palmar direction.

technical problems during preparation of the slide containing the fracture area. Diagnosis: Incomplete nonarticular fracture of proximomedial McIII (diagnostic imaging) with surrounding sclerosis and palmar exostosis (diagnostic imaging and histopathology).

Discussion

The current case describes an incomplete fracture associated with sclerosis and exostosis of the proximal palmar McIII without associated SL involvement diagnosed by nuclear scintigraphy, radiography, ultrasonography, CT and MRI. Palmar cortical fractures, both fatigue and avulsion fractures, have been reported in isolation (Dyson 1991; Riggs 1994; Pinchbeck and Kriz 2001; Morgan and Dyson 2012; Beccati *et al.* 2017) as well as in combination with proximal suspensory desmitis (Ross *et al.* 1988; Beccati *et al.* 2017). Primary osseous injury of the origin of the suspensory ligament with little or no ligamentous pathology has been reported previously (Murray *et al.* 2010) and palmar cortical fatigue fractures have also been identified without ultrasonographic evidence of proximal suspensory desmitis (Dyson 1991). Desmitis of the PSL may be associated with avulsion fractures of McIII at the origin of the suspensory ligament (Launois *et al.* 2003; Zubrod *et al.* 2004) and new bone formation of the palmar aspect of the proximal McIII with concurrent PSL desmitis has also been reported (Launois *et al.* 2009). The authors propose that the exostosis in the current case was due to pre-existing bone injury of this area, as no evidence of desmitis of the PSL was identified.

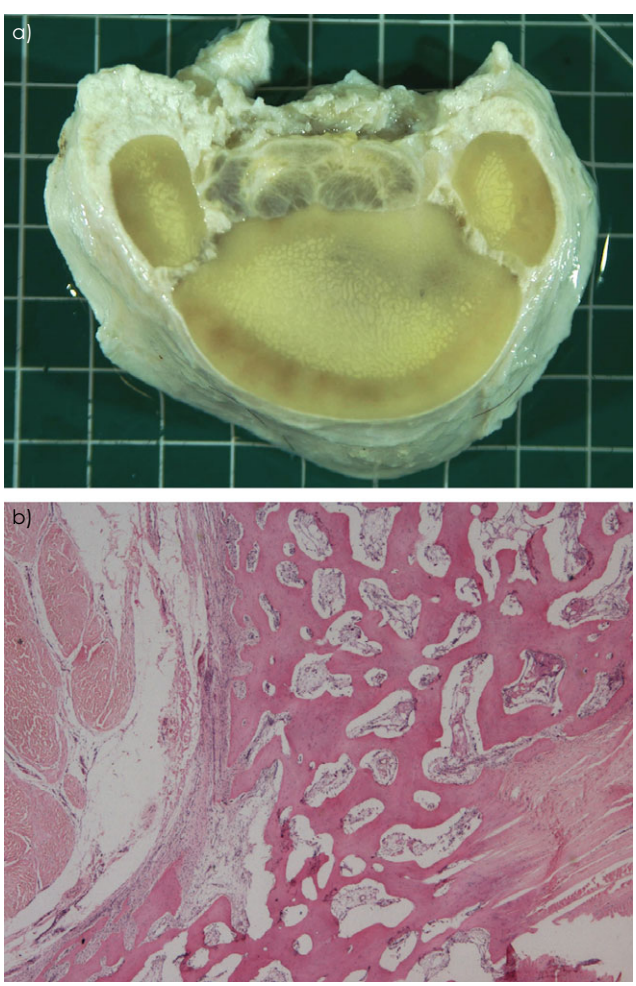

Fig 4: a) Gross post-mortem image of transverse section through McIII. The compact cortical bone of the palmar medial aspect of McIII is thickened and encroaches into the central trabecular bone. The exostosis can be seen abaxial to the suspensory ligament and axial to the McII protruding from the palmar surface of McIII. b) Histopathological section showing the area of focally extensive osteonal bone of the palmar cortex invading the trabecular bone.

A nonweightbearing ultrasound technique (with the carpus in moderate flexion) (Werpy *et al.* 2013) was utilised to allow better contact between the ultrasound probe and the limb. It enabled evaluation of the borders of the PSL as well as examination of a larger proportion of the palmar surface of McIII and axial aspect of McII than weightbearing ultrasonography. This facilitated imaging of the exostosis between the PSL and McII. The bones involved, the full extent of the fracture and the exostosis were further appreciated through cross-sectional imaging (CT and MRI) where it was established that fracture affected McIII rather than McII and revealed the full extent of the exostosis. Earlier reports of similar radiographic findings (before CT or MRI was widely available) documented trabecular hypertrophy and/or medullary sclerosis of the proximal extremity of the McIII but found no evidence of the presence of a fracture (Lloyd *et al.* 1988). Consistent with findings from previous publications (Tucker and Sande 2001; Launois *et al.* 2009; Powell *et al.* 2010; Beccati *et al.* 2017), this case report illustrates how cross-sectional imaging can aid the specific diagnosis of complex injuries in this area especially in cases with inconclusive radiographic findings.

Incomplete fractures at the proximal metacarpus have predominantly, but not exclusively, been identified in racehorses or those undergoing high speed exercise (Morgan and Dyson 2012). MRI in racehorses with subcarpal lameness has identified bone oedema beside palmar cortical thickening (Powell *et al.* 2010) that is likely to represent a different pathological process or a different bone modelling time point (Martig *et al.* 2014) to the current case. Incomplete fractures of the proximal metacarpal region have been reported in a broad spectrum of ages and work disciplines (Morgan and Dyson 2012), and in horses in low levels of work (Riggs 1994; Pinchbeck and Kriz 2001). Medullary sclerosis has been identified by radiography in some, but not all horses, with incomplete fractures of the proximal palmar cortex of McIII (Ross *et al.* 1988) and early bone densification may be undetected in cases where cross-sectional imaging was not performed. The aetiology of the fracture in the current case is not clear. The hypointense signal on T1 FSE images is consistent with sclerosis and the lack of bone oedema suggests chronicity of the lesion beyond the reported 2-week lameness (Ramzan and Powell 2010; Dyson *et al.* 2011). It is plausible that there was pre-existing modelling of the bone in the current case, which resulted in sclerosis and reduced the elasticity of the bone. This process would make the bone more brittle and liable to fracture (Allen and Burr 2013). The occurrence of lameness (only 2-week duration) perhaps coincided with a traumatic event in already brittle bone, which initiated a fracture. The fracture

was identified on radiography and cross-sectional imaging but was not demonstrated on histopathology. The bone proved remarkably dense to section during slide preparation; possibly the fracture gap was lost during specimen processing or the incorrect area was sectioned. However, the sclerotic process was confirmed with histopathology.

The medial aspect appears overrepresented in reports of injuries to the proximal McIII (Lloyd *et al.* 1988; Ross *et al.* 1988; Pleasant *et al.* 1992; Launois *et al.* 2009; Dyson 2011; Morgan and Dyson 2012). One possible explanation for this is because the second carpal bone articulates solely with the second metacarpus, resulting in greater shearing forces of the second metacarpus against the third compared to the fourth metacarpus (Dyson 1988). Two different carpometacarpal articulations have been proposed; Rooney-Prickett type-A carpometacarpal joint configurations where there is no measurable articulation between the third carpal and second metacarpal bones and type-B configurations where there is a measurable articulation between the third carpal and second metacarpal bones (Rooney and Prickett 1966). Medial metacarpal fusion (type-A) has been found to be associated with increasing age, occupation (performance careers) and proportion of the proximal projection of the carpometacarpal distal joint surface that was taken by the second metacarpal bone (Les *et al.* 1995). Another contributing factor of the medial propensity may be the greater proportion of the weight of the horse's trunk distributed along the medial aspect of the limb (Balch *et al.* 1997). MRI of 30 cadaver limbs obtained from nonlame horses found the proximal palmar cortex of the McIII was thicker medially than laterally, suggesting asymmetrical forces act on the limb (Nagy and Dyson 2011). Male horses are overrepresented with incomplete fractures at this location but no genetic or sex linkage has been identified (Ross *et al.* 1988; Morgan and Dyson 2012). The authors propose that the sclerosis in the medial aspect of the proximal McIII may be the result of previous overloading of this area and potentially increased shearing forces.

Conclusion

This is the first report of a palmar fracture of the proximal metacarpus and associated exostosis described by gamma scintigraphy, radiography, ultrasonography, CT and MRI. It demonstrates the valuable information obtained from advanced imaging that allows accurate diagnosis in challenging cases.

Authors' declaration of interests

No conflicts of interest have been declared.

Ethical animal research

The owner of the horse in this case report provided ethical consent for use of case details.

Source of funding

None.

Acknowledgements

We would like to thank the pathology department for help in preparing the histopathology slides.

Authorship

C. M. Isgren and L. M. Rubio-Martinez were involved in the work-up and diagnosis of the case. T. W. Maddox assisted with acquisition and interpretation of advanced imaging and R. Blundell with histopathological interpretation. M. Sinovich provided digital support of all figures. All authors contributed to and gave their final approval of the manuscript.

Manufacturers' addresses

[1]Bartec Technologies, Camberley, UK.
[2]DMS Apelem, Parc Scientifique Georges Besse, Nîmes Cédex 1, France.
[3]GE Medical Systems Ltd, Buckinghamshire, UK.
[4]Siemens, Erlangen, Germany.

References

Allen, M.R. and Burr, D.B. (2013) Chapter 4. Bone modeling and remodeling. In: *Basic and Applied Bone Biology*. Eds: D.B. Burr, M.R. Allen, Elsevier, London.

Arkell, M., Archer, R.M., Guitian, F.J. and May, S.A. (2006) Evidence of bias affecting the interpretation of the results of local anaesthetic nerve blocks when assessing lameness in horses. *Vet. Rec.* **159**, 346-348.

Balch, O.K., Butler, D. and Collier, M.A. (1997) Balancing the normal foot: hoof preparation, shoe fit and shoe modification in the performance horse. *Equine Vet. Educ.* **9**, 143-154.

Beccati, F., Cerocchi, A., Conti, M., Al Pilati, N. and Pepe, M. (2017) Computed tomographic diagnosis of incomplete palmar cortical (fatigue) fracture of the third metacarpal bone in two young adult endurance horses. *Equine Vet. Educ.* Epub ahead of print; https://doi.org/10.1111/eve.12860.

Dyson, S. (1988) Some observations on lameness associated with pain in the proximal metacarpal region. *Equine Vet. J.* **20**, 43-52.

Dyson, S. (1991) Proximal suspensory desmitis: clinical, ultrasonographic and radiographic features. *Equine Vet. J.* **23**, 25-31.

Dyson, S.J. (2011) Chapter 37 - the metacarpal region. In: *Diagnosis and Management of Lameness in the Horse*, 2nd edn., Eds: M.W. Ross, S.J. Dyson, Elsevier, Philadelphia. pp 411-426.

Dyson, S., Nagy, A. and Murray, R. (2011) Clinical and diagnostic imaging findings in horses with subchondral bone trauma of the sagittal groove of the proximal phalanx. *Vet. Radiol. Ultrasound.* **52**, 596-604.

Launois, M.T., Desbrosse, F. and Perrin, R. (2003) Percutaneous osteostixis as treatment for avulsion fractures of the palmar/plantar third metacarpal/metatarsal bone cortex at the origin of the suspensory ligament in 29 cases. *Equine Vet. Educ.* **15**, 126-138.

Launois, M.T., Vandeweerd, J.M.E., Perrin, R.A., Brogniez, L., Desbrosse, F.G. and Clegg, P.D. (2009) Use of computed tomography to diagnose new bone formation associated with desmitis of the proximal aspect of the suspensory ligament in third metacarpal or third metatarsal bones of three horses. *J. Am. Vet. Med. Assoc.* **234**, 514-518.

Les, C.M., Stover, S.M. and Willits, N.H. (1995) Necropsy survey of metacarpal fusion in the horse. *Am. J. Vet. Res.* **56**, 1421-1432.

Lloyd, K.C., Koblik, P., Ragle, C., Wheat, J.D. and Lakritz, J. (1988) Incomplete palmar fracture of the proximal extremity of the third metacarpal bone in horses: ten cases (1981-1986). *J. Am. Vet. Med. Assoc.* **192**, 798-803.

Martig, S., Chen, W., Lee, P.V.S. and Whitton, R.C. (2014) Bone fatigue and its implications for injuries in racehorses. *Equine Vet. J.* **46**, 408-415.

Morgan, R. and Dyson, S. (2012) Incomplete longitudinal fractures and fatigue injury of the proximopalmar medial aspect of the third metacarpal bone in 55 horses. *Equine Vet. J.* **44**, 64-70.

Murray, R.C., Brokken, M.T. and Tucker, R.L. (2010) Chapter 14 - The metacarpal/metatarsal region. In: *Equine MRI*. 1st edn., Eds: R.C. Murray, John Wiley & Sons, Chichester.

Nagy, A. and Dyson, S. (2011) Magnetic resonance imaging and histological findings in the proximal aspect of the suspensory ligament of forelimbs in nonlame horses. *Equine Vet. J.* **44**, 43-50.

Pinchbeck, G.L. and Kriz, N.G. (2001) Two cases of complete longitudinal fracture of the proximopalmar aspect of the third metacarpal bone. *Equine Vet. Educ.* **13**, 187-193.

Pleasant, R.S., Baker, G.J., Muhlbauer, M.C., Foreman, J.H. and Boero, M.J. (1992) Stress reactions and stress fractures of the proximal palmar aspect of the third metacarpal bone in horses: 58 cases (1980-1990). *J. Am. Vet. Med. Assoc.* **201**, 1918-1923.

Powell, S.E., Ramzan, P.H.L., Head, M.J., Shepherd, M.C., Baldwin, G.I. and Steven, W.N. (2010) Standing magnetic resonance imaging detection of bone marrow oedema-type signal pattern associated with subcarpal pain in 8 racehorses: a prospective study. *Equine Vet. J.* **42**, 10-17.

Ramzan, P.H.L. and Powell, S.E. (2010) Clinical and imaging features of suspected prodromal fracture of the proximal phalanx in three Thoroughbred racehorses. *Equine Vet. J.* **42**, 164-169.

Riggs, C.M. (1994) Incomplete fracture of the proximo-palmar aspect of the third metacarpal bone. *Equine Vet. Educ.* **6**, 263-267.

Rooney, J.R. and Prickett, M.E. (1966) Foreleg splints in horses. *Cornell. Vet.* **56**, 259-269.

Ross, M.W., Ford, T.S. and Orsini, P.G. (1988) Incomplete longitudinal fracture of the proximal palmar cortex of the third metacarpal bone in horses. *Vet. Surg.* **17**, 82-86.

Tucker, R.L. and Sande, R.D. (2001) Computed tomography and magnetic resonance imaging in equine musculoskeletal conditions. *Vet. Clin. North Am. Equine Pract.* **17**, 145-157.

Werpy, N.M., Denoix, J.M., McIlwraith, C.W. and Frisbie, D.D. (2013) Comparison between standard ultrasonography, angle contrast ultrasonography, and magnetic resonance imaging characteristics of the normal equine proximal suspensory ligament. *Vet. Radiol. Ultrasound.* **54**, 536-547.

Zubrod, C.J., Schneider, R.K. and Tucker, R.L. (2004) Use of magnetic resonance imaging to identify suspensory desmitis and adhesions between exostoses of the second metacarpal bone and the suspensory ligament in four horses. *J. Am. Vet. Med. Assoc.* **224**, 1815-1820.